Annals of Nuclear Medicine Vol. 18, No. 3, 195–202, 2004

Abnormal retention of ^{99m}Tc-TF in a hamster model of cardiomyopathy analyzed by ^{99m}Tc-TF and ^{125}I-BMIPP autoradiography

Thet-Thet-Lwin, Tohoru Takeda, Jin Wu, Yoshinori Tsuchiya and Yuji Itai

*Graduate School of Comprehensive Human Sciences, University of Tsukuba

Objective: Enhanced washout of ^{99m}Tc-tetrofosmin (TF) has been reported in patients with hypertrophic cardiomyopathy (HCM). Here, using quantitative dual-autoradiography, the relationship between TF retention abnormality and metabolism depicted by ^{125}I-BMIPP uptake was investigated quantitatively in a hamster model of cardiomyopathy. ***Methods and Results:*** Early and delayed TF images were obtained at 5 min (7 cardiomyopathic and 5 normal hamsters) and 60 min (8 cardiomyopathic and 5 normal hamsters) after injection, respectively. BMIPP image was obtained 5 min after injection. Five cardiomyopathic and 5 normal hamsters were evaluated histologically. Percent uptake of TF and BMIPP in the heart was measured by an auto-well counter. The left ventricular wall was divided into 12 segments, and the relative regional uptake of TF and BMIPP was measured for each segment. Heterogeneity of radioactive distribution was determined by the standard deviation (SD) of radioactive counts in the left ventricular wall on autoradiogram. The uptake of early TF, delayed TF, and BMIPP in cardiomyopathic hamsters was 8.8%, 20.3%, and 25.3% lower than that in normal hamsters, $p < 0.05$, $p < 0.01$, and $p < 0.001$, respectively. In normal hamsters, distribution of radioactivity in all images was homogeneous, and the SD values were about 13. In cardiomyopathic hamsters, heterogeneous distribution was observed on all images, and the degree of heterogeneity was marked on delayed TF and BMIPP images. The SD was 19.7 ± 1.2 for early TF image, 25.5 ± 1.4 for delayed TF image, and 31.7 ± 2.4 for BMIPP image, respectively. A weak linear correlation was observed between the relative regional uptake of the delayed TF and BMIPP in cardiomyopathic hamsters ($r = 0.57$). Electron microscopy demonstrated ultra-structural changes in mitochondria of cardiomyopathic hamsters. ***Conclusion:*** Degree of retention abnormality on delayed TF image corresponded to the metabolic abnormality, probably due to mitochondrial dysfunction, depicted on BMIPP imaging.

Key words: autoradiography, ^{99m}Tc-TF, ^{125}I-BMIPP, cardiomyopathy, myocardial metabolism

INTRODUCTION

Lipophilic, cationic diphosphine complex ^{99m}Tc-tetrofosmin (TF) is one of the most useful radionuclide agents to evaluate myocardial perfusion.[1,2] TF, which accumulates rapidly in myocardium after injection, was reportedly retained there for a long time without washout.[3,4] However, enhanced washout of TF has been recently found in acute myocardial infarction,[5,6] complete left bundle branch block,[7] and hypertrophic cardiomyopathy (HCM).[8,9] This enhanced washout of TF is considered to be caused by metabolic abnormality. We have found that the degree of TF washout corresponds well to that of both myocardial wall thickness and metabolic abnormality as seen with ^{123}I-β-methyl-*p*-iodophenylpentadecanoic acid (^{123}I-BMIPP) in patients with HCM.[10]

The present study was undertaken to investigate the occurrence and degree of retention abnormality of TF in an animal model of HCM (J2N-k Syrian hamster) using dual autoradiographic technique with TF and ^{125}I-BMIPP.

Received July 29, 2003, revision accepted January 16, 2004.

For reprint contact: Tohoru Takeda, M.D., Ph.D, Graduate School of Comprehensive Human Sciences, University of Tsukuba, Tennodai 1–1–1, Tsukuba, Ibaraki 305–8575, JAPAN.

E-mail: ttakeda@md.tsukuba.ac.jp

MATERIALS AND METHODS

Animal model

Cardiomyopathic Syrian hamster J2N-k and non-cardiomyopathic hamster J2N-n were obtained by various cross breeding between Bio 14.6 cardiomyopathic Syrian hamster and Golden hamster. Bio 14.6 develops myocardial hypertrophy at three to four months of age and marked cardiac dilatation around six months of age, preceding death due to congestive cardiac failure.[11–14] At the stage of hypertrophy, focal necrosis develops at one month of age, followed by fibrosis and small calcification at three to four months of age. Compared with the Bio 14.6, the pathologic development of J2N-k is slower and milder in nature. The main feature of cardiomyopathy changes in J2N-k is the lack of focal myocardial necrosis observed in Bio 14.6. In addition, the development of interstitial fibrosis is slower, and the elevation of serum enzyme level is less severe in J2N-k of the same age.[15,16] Therefore, J2N-k was used as an animal model for human cardiomyopathy.

Twelve-week-old J2N-k cardiomyopathic hamsters were divided into two groups as early (n = 7) and delayed (n = 8). Five age-matched J2N-n hamsters were used as a normal control for each group. The care and use of laboratory animals in this study were in accordance with the guidelines and regulations issued by Tsukuba University.

Radioactive TF and BMIPP uptake

Five mCi (185 MBq) of TF and 50 μCi (1.85 MBq) of BMIPP were injected at the same time to the early group, and the hearts were extracted at 5 min after the injection. In the delayed group, 5 mCi (185 MBq) of TF was injected first, and 50 μCi (1.85 MBq) of BMIPP was injected 55 min later. The hearts were extracted 5 min after the second injection.

The hearts were excised and weighed. Using an auto-well counter (ARC-300, Aloka, Tokyo, Japan) with a set of different energy windows (20–40 keV for BMIPP, 140 keV for TF), myocardial count and injected dose count of TF, and BMIPP were measured. After correction to physical decay of ^{99m}Tc, percent uptake of TF and BMIPP was calculated by using the following formula:

$$\%\ \text{uptake (\%ID/g)} = (\text{heart counts/injection dose counts/heart weight}) \times 100$$

Autoradiography

In dual autoradiographic study, the second exposure should be conducted after adequate time for decay of the first tracer. Therefore, ^{99m}Tc, which has a short half-life of 6 hr, was used with ^{125}I, which has 60 days half-life, which is longer than the 13-hr half-life of ^{123}I for our study.

After counting the myocardial radioactivity, the hearts

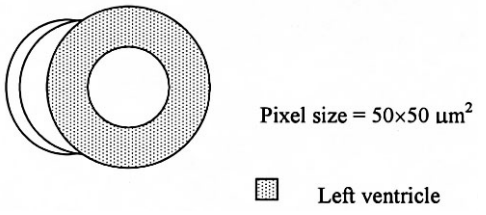

Fig. 1 Left ventricle was demarcated manually on autoradiogram.

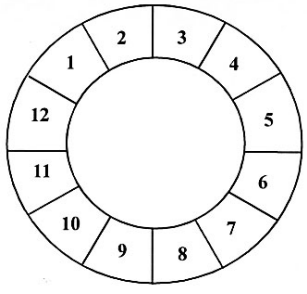

Fig. 2 Diagram of standard segmentation scheme used for relative regional uptake analysis in autoradiography.

Table 1 Mean pixel numbers of left ventricle in normal and cardiomyopathic hamsters

	Normal hamsters		Cardiomyopathic hamsters	
	Early (n = 5)	Delayed (n = 5)	Early (n = 7)	Delayed (n = 8)
Mean pixel numbers	15836 ± 207	15722 ± 220	16080 ± 432	16037 ± 544

Table 2 Percent radioactive uptake (%ID/g) in normal and cardiomyopathic hamsters on early TF, delayed TF, and BMIPP images

	Early TF images	Delayed TF images	BMIPP images
Normal hamsters	1.58 ± 0.05	1.53 ± 0.09	5.34 ± 0.32
Cardiomyopathic hamsters	1.44 ± 0.09	1.22 ± 0.14	3.99 ± 0.74
% Difference of normal and cardiomyopathic hamsters	8.8	20.3	25.3

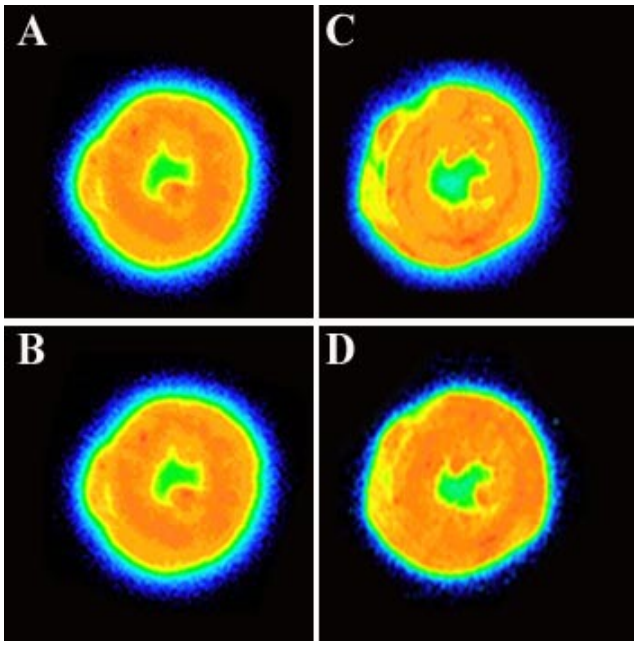

Fig. 3 Autoradiographic image with TF (*top*) and BMIPP (*bottom*) in the normal hamsters. Radionuclide agents distributed almost homogeneously in (A) 5 min TF image, (B) 5 min BMIPP image (the same section of A), (C) TF 1 hr image, and (D) 5 min BMIPP image (the same section as C).

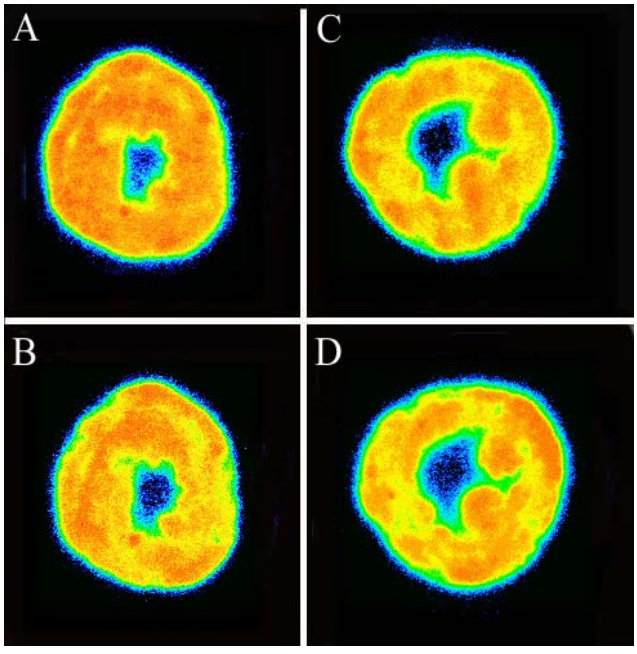

Fig. 4 Autoradiographic image with TF (*top*) and BMIPP (*bottom*) in cardiomyopathic hamsters. (A) 5 min TF image shows a slightly decreased distribution. (B) 5 min BMIPP image (the same section as A) shows markedly patchy and decreased uptake. Similar pattern of markedly patchy and decreased uptake on (C) 1 hr TF image (D) 5 min BMIPP image (the same section as C).

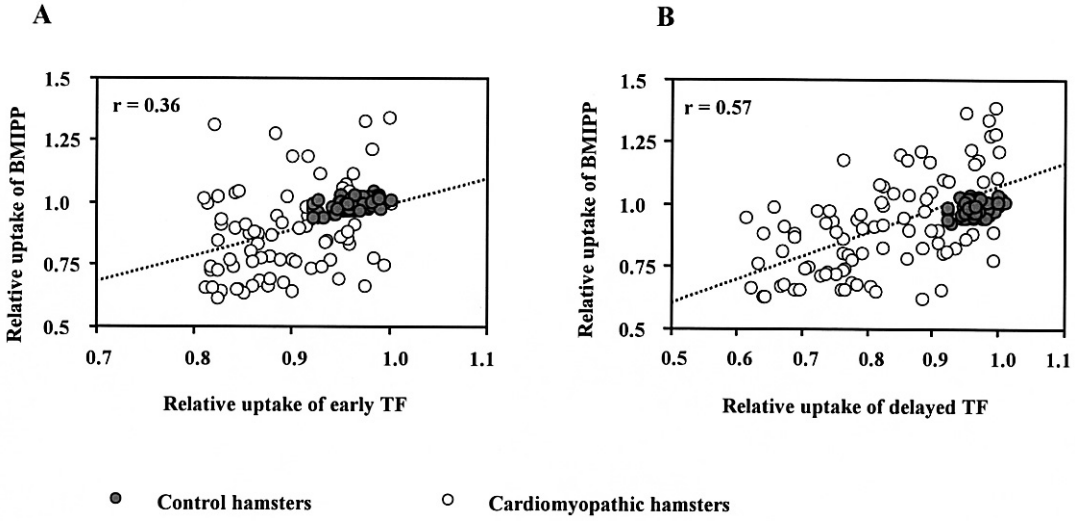

Fig. 5 Correlation between the relative regional uptake of early TF and BMIPP in control and cardiomyopathic hamsters (A). Correlation between the relative regional uptake of delayed TF and BMIPP in control and cardiomyopathic hamsters (B).

were frozen in isopentane, which had been cooled in dry ice, and embedded in methylcellulose. Specimens were sliced along the short axis at mid-ventricle level. Each specimen was sliced at 50 μm thickness for macro-autoradiography using a cryomicrotone (CM3050 V1.3 Espanol, Germany) at −20°C.

The myocardial sections were exposed to an imaging plate (BAS-SR 2025; Fuji Photo Film Co., Ltd., Tokyo, Japan). The first autoradiographic image was obtained within one hour of heart extraction to visualize the TF distribution. Thirty days later, following the complete decay of ^{99m}Tc activity, the second image of the same

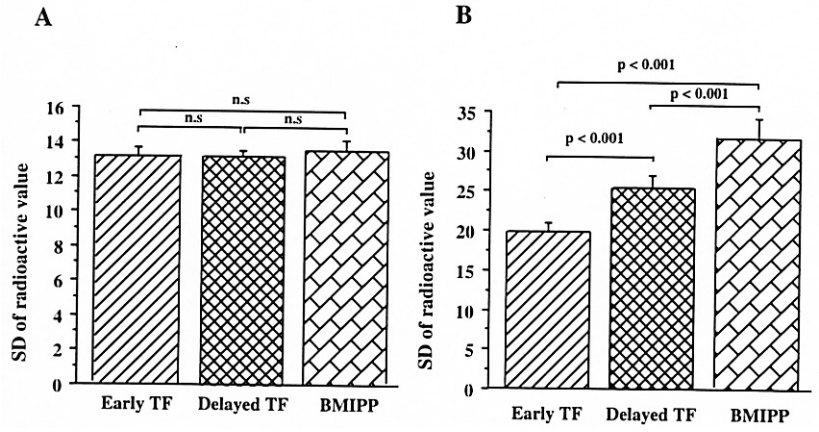

Fig. 6 Standard deviation of TF and BMIPP radioactive values in normal hamsters (A) and cardiomyopathic hamsters (B).

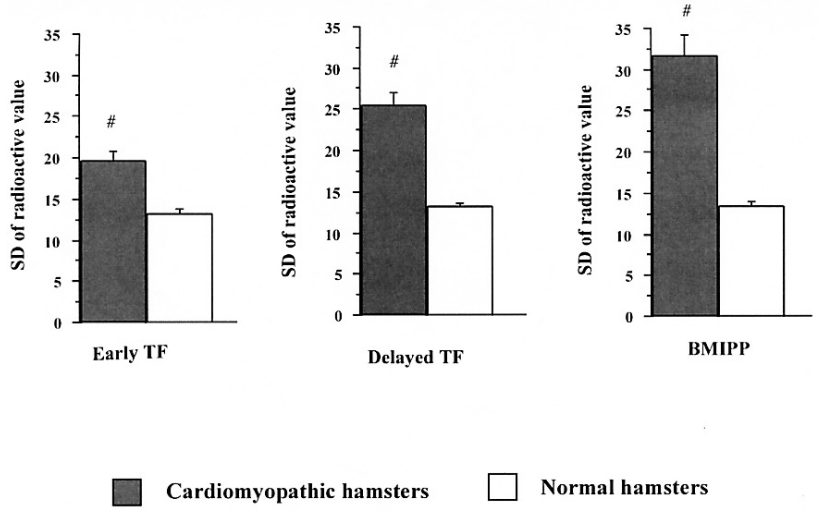

Fig. 7 Comparison of standard deviation of radioactivity between the normal and cardiomyopathic hamsters on early TF, delayed TF, and BMIPP images. # $p < 0.001$ to normal hamsters.

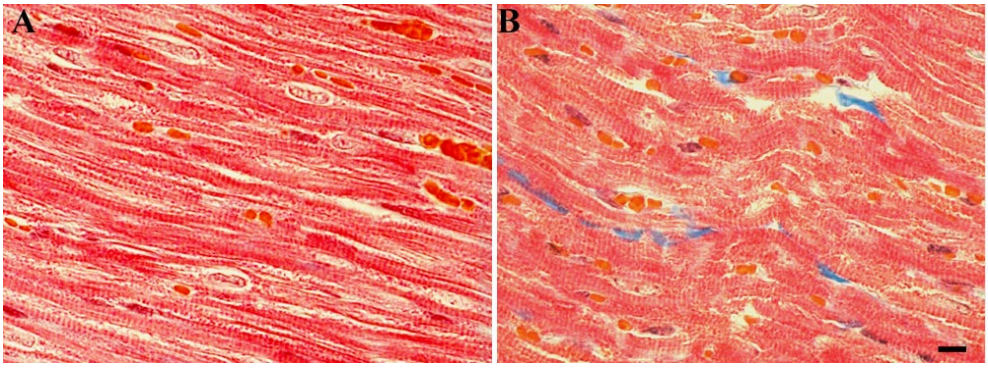

Fig. 8 Light microscopy with Masson's trichrome staining shows no fibrotic changes in normal hamster (A) and slight interstitial fibrosis in cardiomyopathic hamster (B). Bar = 20 μm

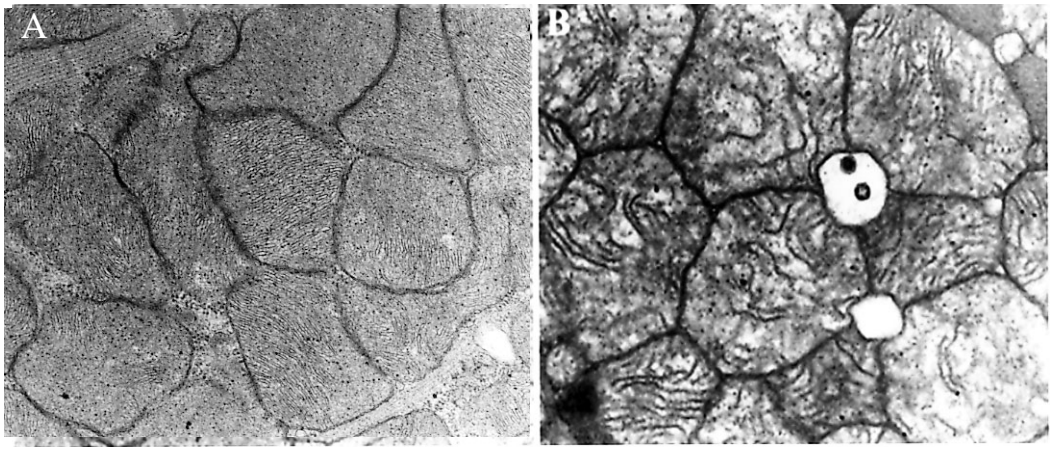

Fig. 9 Electron microscopy shows normal mitochondrial findings in a normal hamster (A) and mitochondrial changes such as alteration in size and shape, clustering appearance and changes in cristae pattern in a cardiomyopathic hamster (B). × 20,000

section was exposed for two weeks to visualize the BMIPP distribution. In the preliminary study, single tracer autoradiography with TF and BMIPP under the same imaging condition as dual tracer autoradiography was performed to confirm the non-visualization of an overlapping effect of the two tracers.

Digital autoradiographic images were obtained using a Bio imaging Analysis System (BAS) 5000 (Fuji Photo Film Co., Ltd., Japan) with a pixel size of $50 \times 50\ \mu m^2$ and a 16 bits resolution. For the precise measurement of tracer uptake on autoradiographic images, the left ventricle was demarcated manually (Fig. 1), and the accumulation of radioactive agents was measured on each image. Heterogeneity of radioactive distribution was expressed by the standard deviation (SD) of the regional pixel uptake in left ventricle. The mean pixel numbers of normal and control hamsters were shown in Table 1.

In addition, the left ventricle wall was divided into twelve segments to analyze the relationship between the relative regional uptake of TF and BMIPP as shown in Figure 2. The mean uptake in these selected regions was measured. In the TF images, the relative uptake of the tracer for each region was defined as the ratio of the regional count normalized by the maximal count in the twelve regions. In the BMIPP images, the relative uptake of the tracer was calculated as the ratio of the regional count normalized by the count of region, which is the maximal count in the TF image.

Histology

Histological evaluation was performed on twelve-week-old cardiomyopathic hamsters (n = 5) and normal hamsters (n = 5). Following rapid removal of the heart, ventricular slices (approximately 1–2 mm thick and 3–4 mm in diameter) were immersed in fixative and sliced into 1-mm cubes. Primary fixation was done for 2–4 hr in 2.5% glutaraldehyde in 0.1 M phosphate buffer, pH 7.4. Tissue were fixed for 2 hr in cold, buffered 1% OsO_4, and dehydrated in a graded series of ethanol and propylene oxide, and embedded in Epon. Remaining heart tissues, which were not processed for electron microscopy, were fixed with 10% buffered formalin, embedded in paraffin wax, and then sectioned and stained with Masson's trichrome (MT) for light microscopy. Semithin sections of Epon-embedded blocks were cut on Reichert—Jung ultramicrotomes, and stained with toluidine blue. Thin sections were cut on the Reichert—Jung microtome with a diamond knife, stained with uranyl acetate and lead citrate, and examined at 75 kV in a Hitachi (H-7000) electron microscope.

Statistical analysis

All radioactive counts were expressed as mean ± standard deviation. Data were analyzed by unpaired student *t* tests. A p value less than 0.05 was considered to indicate statistical significant difference.

RESULTS

Myocardial uptake of TF and BMIPP

Percent myocardial uptake of TF and BMIPP in normal and cardiomyopathic hamsters is shown in Table 2. In normal hamsters, no significant difference was observed between the early TF uptake and delayed TF uptake (1.58 ± 0.05 vs. 1.53 ± 0.09). However, in cardiomyopatic hamsters, the early TF uptake was significantly higher than the delayed TF uptake (1.44 ± 0.09 vs. 1.22 ± 0.14, $p < 0.05$). Early TF uptake and delayed TF uptake in cardiomyopathic hamsters were 8.8% ($p < 0.05$) and 20.3% ($p < 0.01$) less than that in normal hamsters, respectively. BMIPP uptake of cardiomyopathic hamsters was 25.3% less than that of normal hamsters ($p < 0.001$).

Autoradiography

In the normal control hamsters, the early TF, delayed TF and BMIPP distributions were almost homogeneous as shown in Figure 3. However, in the cardiomyopathic hamsters (Fig. 4), the early TF image showed a slightly heterogeneous distribution, while the same section of the BMIPP image showed a significantly heterogeneous distribution. Besides, quite a similar heterogeneous distribution was observed in the delayed TF image and BMIPP image.

Using the analysis of 12 left ventricular myocardial segments, the correlations between the relative BMIPP uptake and the TF uptake (early and delayed) were shown in Figure 5 (A and B). In the normal control hamsters, a small range of distribution was observed between TF and BMIPP both on early and delayed images, and the mean relative regional uptakes of early TF, delayed TF and BMIPP were 0.97 ± 0.02, 0.96 ± 0.02, and 0.99 ± 0.03, respectively. In cardiomyopathic hamsters, a wide range of distribution was observed between TF and BMIPP both on early and delayed images, and the mean relative uptakes of early TF, delayed TF and BMIPP were 0.90 ± 0.06, 0.83 ± 0.11, and 0.90 ± 0.18, respectively. No correlation was seen between the relative early TF uptake and the relative BMIPP uptake ($r = 0.36$), whereas a weak positive correlation was seen between the relative delayed TF uptake and the relative BMIPP uptake ($r = 0.57$).

The heterogeneity of radioactivity was analyzed by using the SD of radioactive uptake on autoradiography. The SD values of early TF, delayed TF, and BMIPP images in the normal hamsters were 13.1 ± 0.4, 13.2 ± 0.3, and 13.5 ± 0.6, respectively, and all values were almost the same (Fig. 6A). In cardiomyopathic hamsters, however, the SD value of early TF image (19.7 ± 1.2) was smaller than that of the delayed TF image (25.5 ± 1.4) and the BMIPP image (31.7 ± 2.4) (Fig. 6B). The SD values of early TF image and delayed TF image in cardiomyopathic hamsters were 1.5 times and 1.9 times larger than that in normal hamsters, $p < 0.001$ and $p < 0.001$, respectively. In BMIPP image, the SD value of the cardiomyopathic hamsters was 2.3 times larger than that of the normal hamsters ($p < 0.001$) (Fig. 7).

Histological findings

In light microscopy with Masson's trichrome (MT) staining, slight interstitial fibrosis was seen in cardiomyopathic hamsters while there were no fibrotic changes in normal hamsters (Fig. 8). Besides, by electron microscopy, mitochondrial changes such as alterations in size and shape, clustering appearance, and changes in the cristae pattern were observed in cardiomyopathic hamsters, while no abnormalities were seen in the normal hamsters (Fig. 9).

DISCUSSION

Decreased uptake and heterogeneous distribution were observed on delayed TF images and BMIPP images of cardiomyopathic hamsters.

Myocardial uptake of TF and BMIPP

The percent myocardial uptake of early TF (1.6%) and BMIPP (5.3%) in normal hamsters is similar to the previous reported uptake of 1.7% in Wistar rat at 2-min TF[1] and 6.8% in rat at 5-min BMIPP.[17] There was no significant difference between early image of 1.6% and delayed image of 1.5% in normal hamsters, whereas the percent myocardial uptakes of the early TF (1.4%), delayed TF (1.2%), and BMIPP (3.9%) in the cardiomyopathic hamsters were significantly lower than the respective values in the normal hamsters. In addition, the delayed TF uptake was significantly lower than the early TF uptake. Therefore, the retention abnormality appeared to occur in early and delayed TF images, and the degree of abnormality was marked in the delayed images.

Autoradiography

In normal hamsters, the radioactive distribution on macroautoradiographic image was almost homogeneous on early TF image, delayed TF image and BMIPP image, and the degree of heterogeneity expressed by SD value was about 13 in all images. However, in cardiomyopathic hamsters, mild heterogeneity was observed on early TF image and its degree became more obvious on delayed TF image, resulting in an increment of SD values from 19.7 to 25.5. BMIPP image showed a significant heterogeneous distribution, and the SD value was 31.7.

The pattern of heterogeneous distribution observed on delayed TF images and BMIPP images was quite similar; however the degree of heterogeneity in delayed TF appeared to be underestimated. Using data from 12 segment autoradiographic analysis in cardiomyopathic hamsters, a weak linear correlation was observed between the relative regional uptake on the delayed TF and that on BMIPP, whereas no relationship was observed between the relative regional uptake on the early TF and that on BMIPP. It is considered that the image acquisition time (one hour) of delayed TF image should be shortened to obtain the consistent images of BMIPP because washout of TF occurs with time.

Histological consideration

In cardiomyopathic hamsters, the degree of fibrosis was mild in myocardium, however moderately decreased uptake and heterogeneity were observed on TF images, especially on delayed TF image. These results indicate that reduced uptake of TF was caused by the retention abnormality rather than the reduced myocardial mass density due to fibrotic changes. The retention of TF was reported to be reduced by metabolic inhibitors (such as 2,4-dinitrophenol and carbonyl cyanide *m*-chlorophenylhydrazone).[18–21] Therefore, to investigate the possible reason for the TF retention abnormality, we used BMIPP

as a marker of metabolic alteration because the degree of BMIPP uptake is closely reflected by the myocardial ATP concentration,[22,23] and mitochondrial and cell membrane functions.[24] The observed heterogeneity and reduced uptake of BMIPP similar to TF in this study might be caused by the impaired cellular and mitochondrial function with limited ATP generation. Actually, ultrastructural changes in mitochondria of cardiomyopathic hamster's myocardium were observed by electron microscopy. In addition, impaired phosphorylation caused by decreased ADP/ATP carrier protein on the inner membrane of the mitochondria has been reported previously in J2N-k cardiomyopathy hamsters.[25] Furthermore, the excess Ca^{2+} influx is reported to reduce TF retention,[18,20,21] and the increased accumulation of Ca^{2+} in myocyte is induced by the depressed sarcolemmal Na^+K^+ ATPase, Ca^{2+} ATPase and Na^+/Ca^{2+} exchange in J2N-k cardiomyopathic hamster's myocardium.[26] Although we have not examined Ca^{2+} influx in this study, the reduced retention of TF might be affected partially by Ca^{2+} overload.

The area and degree of retention abnormality on delayed TF image were corresponded closely to those of metabolic abnormality on the BMIPP image probably due to mitochondrial dysfunction. Therefore, the retention abnormality, which occurred especially in delayed TF image, might be affected by the metabolic alteration in cardiomyopathic myocardium.

Study limitations

In this study, we set delayed image at one hr based on a previous animal study.[27] However, the degree of metabolic abnormality in the delayed TF image appeared to be underestimated. If the delayed image had been obtained much later, the degree of TF uptake might be more similar to that of BMIPP because the uptake of TF decreases with time. The combined study of the TF delayed image and quantitative washout analysis should provide additional information concerning metabolic abnormalities in cardiomyopathy. *In vivo* imaging with quantitative washout analysis of TF by using animal SPECT equipment would be needed in future studies.

Histological examination was not performed on the same animal used for autoradiography because specimens are not allowed to be taken out of the radioisotope department for histological examination.

CONCLUSION

The decreased uptake observed on the delayed TF image is a reliable marker for metabolic alteration, and a single injection of TF could be used not only to evaluate perfusion abnormalities but also to estimate the metabolic alterations in HCM.

ACKNOWLEDGMENTS

The authors thank Dr. Shinji Sugahara, Ms. Junko Sakamoto, Ms. Takako Fukaya, Ms. Yasuko Fukunaka, and Ms. Hiroko Kikukawa for their help with the histological examination, and Ms. Yukiko Kawata for preparation of the manuscript. In addition, we are grateful to Nihon Medi-Physics Co., Ltd. Japan for supplying ^{125}I-BMIPP, and the Radio Isotope Department of Tsukuba University for general help with this research.

REFERENCES

1. Kelly JD, Forster AM, Higley B, Archer CM, Booker FS, Canning LR, et al. Technetium-99m-tetrofosmin as a new radiopharmaceutical for myocardial perfusion imaging. *J Nucl Med* 1993; 34: 222–227.
2. Rigo P, Leclercq B, Itti R, Lahiri A, Braat S. Technetium-99m-tetrofosmin myocardial imaging: a comparison with thallium-201 and angiography. *J Nucl Med* 1994; 35: 587–593.
3. Sridhara BS, Braat S, Rigo P, Itti R, Cload P, Lahiri A. Comparison of myocardial perfusion imaging with technetium-99m tetrofosmin versus thallium-201 in coronary artery disease. *Am J Cardio*l 1993; 72: 1015–1019.
4. Nakajima K, Taki J, Shuke N, Bunko H, Takata S, Hisada K. Myocardial perfusion imaging and dynamic analysis with technetium-99m tetrofosmin. *J Nucl Med* 1993; 34: 1478–1484.
5. Sugihara H, Nakagawa T, Yamashita E, Kinoshita N, Ito K, Azuma A, et al. Reverse redistribution of Tc-99m-tetrofosmin in patients with acute myocardial infarction. *Ann Nucl Med* 1999; 13: 43–47.
6. Tanaka R, Nakamura T. Time course evaluation of myocardial perfusion after reperfusion therapy by ^{99m}Tc-tetrofosmin SPECT in patients with acute myocardial infarction. *J Nucl Med* 2001; 42: 1351–1358.
7. Sugihara H, Kinoshita N, Adachi Y, Taniguchi Y, Ohtsuki K, Azuma A, et al. Early and delayed Tc-99m-tetrofosmin myocardial SPECT in patients with left bundle branch block. *Ann Nucl Med* 1998; 12: 281–286.
8. Sugihara H, Taniguchi Y, Kinoshita N, Nakamura T, Hirasaki S, Azuma A, et al. Reverse redistribution of Tc-99m-tetrofosmin in exercise myocardial SPECT in patients with hypertrophic cardiomyopathy. *Ann Nucl Med* 1998; 12: 287–292.
9. Morishita S, Kondo Y, Nomura M, Miyajima H, Nada T, Ito S, et al. Impaired retention of technetium-99m tetrofosmin in hypertrophic cardiomyopathy. *Am J Cardiol* 2001; 87: 743–747.
10. Thet-Thet-Lwin, Takeda T, Wu J, Fumikura Y, Iida K, Kawano S, et al. Enhanced washout of ^{99m}Tc-tetrofosmin in hypertrophic cardiomyopathy: Quantitative comparisons with regional ^{123}I-BMIPP uptake and wall thickness determined by MRI. *Eur J Nucl Med Mol Imaging* 2003; 30: 966–973.
11. Homburger F, Baker JR, Nixon CW, Whitney R. Primary generalized polymyopathy and cardiac necrosis in an inbred line of Syrian hamsters. *Med Exp* 1962; 6: 339–345.
12. Bajusz E, Baker JR, Nixon CW, Homburger F. Spontaneous hereditary myocardial degeneration and congestive heart failure in a strian of Syrian hamsters. *Ann NY Acad Sci*

1969; 156: 105–129.
13. Bishop SP, Sole MJ, Tilley LP. Cardiomyopathies. In: *Spontaneous models of human disease*. Andrews EJ, Ward BC, Altman NH (eds), New York; Academic Press, 1979: 59–64.
14. Gertz EW. Cardiomyopathic Syrian hamster: a possible model of human disease. *Prog Exp Tumor Res* 1972; 16: 242–260.
15. Nagano M, Takeda N, Kato M, Nagai M, Yang J. Pathophysiologic aspects of cardiomyopathic J-2-N hamsters. In: *The cardiomyopathic heart*. Nagano M, Takeda N, Dhalla N (eds), New York; Raven Press, 1994: 65–72.
16. Kato M, Takeda N, Yang J, Nagano M. The effects of angiotensin converting enzyme inhibitors and the role of the renin-angiotensin-aldosterone system in J-2-N cardiomyopathic hamsters. *Jpn Circ J* 1992; 56: 46–51.
17. Morishita S, Kusuoka H, Yamamichi Y, Suzuki N, Kurami M, et al. Kinetics of radioiodinated species in subcellular fraction from rat hearts following administration of iodine-123-labelled 15-(*p*-iodophenyl)-3-(*R*,*S*)-methylpentadecanoic acid (^{123}I-BMIPP). *Eur J Nucl Med* 1996; 23: 383–389.
18. Platts EA, North TL, Pickett RD, Kelly JD. Mechanism of uptake of technetium-tetrofosmin. I: Uptake into isolated adult rat ventricular myocytes and subcellular localization. *J Nucl Cardiol* 1995; 2: 317–326.
19. Younes A, Songadele JA, Maublant J, Platts E, Pickett R, Veyre A. Mechanism of uptake of technetium tetrofosmin. II: Uptake into adult rat heart mitochondria. *J Nucl Cardiol* 1995; 2: 327–333.
20. Arbab AS, Koizumi K, Toyama K, Araki T. Uptake of technetium-99m-tetrofosmin, technetium-99m-MIBI and thallium-201 in tumor cell lines. *J Nucl Med* 1996; 37: 1551–1556.
21. Arbab AS, Koizumi K, Toyama K, Arai T, Araki T. Technetium-99m-tetrofosmin, technetium-99m-MIBI and thallium-201 uptake in rat myocardial cells. *J Nucl Med* 1998; 39: 266–271.
22. Fujibayashi Y, Yonekura Y, Takemura Y, Wada K, Matsumoto K, Tamaki N, et al. Myocardial accumulation of iodinated beta-methyl-branched fatty acid analogue, iodine-125-15-(*p*-iodophenyl)-3-(*R*,*S*)methylpentadecanoic acid (BMIPP), in relation to ATP concentration. *J Nucl Med* 1990; 31: 1818–1822.
23. Fujibayashi Y, Yonekura Y, Tamaki N, Yamamoto K, Som P, Knapp FF, et al. Myocardial accumulation of BMIPP in relation to ATP concentration. *Ann Nucl Med* 1993; 7 (Suppl II): s15–18.
24. Ogata M. Myocardial uptake of ^{125}I-BMIPP in rats treated with adriamycin. *KAKU IGAKU (Jpn J Nucl Med)* 1989; 26: 69–76.
25. Yan J, Kato M, Takeda N, Nagano M. ADP/ATP carrier proteins in J-2-N cardiomyopathic hamster. *J Mol cell Cardiol* 1992; 24 [suppl I]: s6–16.
26. Kato M, Nagai M, Ohkubo T, Nagano M. Perturbation of calcium transport system of cardiomyopathic Syrian hamster. *J Mol Cell Cardiol* 1989; 21 (Suppl II): s82-245.
27. Takahashi N, Reinhardt CP, Marcel R, Leppo JA. Myocardial uptake of ^{99m}Tc-tetrofosmin, sestamibi, and ^{201}Tl in a model of acute coronary reperfusion. *Circulation* 1996; 15: 2605–2613.